Accepted Manuscript

External CFRP tendon members: Secondary reactions and moment redistribution

Tiejiong Lou, Sergio M.R. Lopes, Adelino V. Lopes

PII: S1359-8368(13)00585-4
DOI: http://dx.doi.org/10.1016/j.compositesb.2013.10.010
Reference: JCOMB 2687

To appear in: *Composites: Part B*

Received Date: 10 June 2013
Revised Date: 21 September 2013
Accepted Date: 14 October 2013

Please cite this article as: Lou, T., Lopes, S.M.R., Lopes, A.V., External CFRP tendon members: Secondary reactions and moment redistribution, *Composites: Part B* (2013), doi: http://dx.doi.org/10.1016/j.compositesb.2013.10.010

External CFRP tendon members: Secondary reactions and moment redistribution

Tiejiong Lou[1], Sergio M. R. Lopes[*1], Adelino V. Lopes[2]

1. CEMUC, Department of Civil Engineering, University of Coimbra, Coimbra 3030-788, Portugal
2. Department of Civil Engineering, University of Coimbra, Coimbra 3030-788, Portugal
(*) – Corresponding author, email: sergio@dec.uc.pt; tel.: +351-239797253

Abstract: The response of prestress secondary reactions in the post-elastic range has been a topic of much controversy. Due to the brittleness of FRP (fiber reinforced polymer) composites, external FRP tendon members may have different moment redistribution characteristics compared to conventional concrete members. This paper presents a numerical investigation into the secondary reactions and moment redistribution in prestressed concrete continuous members with external CFRP tendons. The investigation parameters include the initial prestress level and the pattern of loading. The secondary reactions are computed using a newly developed method based on the linear transformation concept combined with a nonlinear finite element analysis. The results indicate that the secondary reactions increase quicker after concrete cracking and nonprestressed steel yielding. As a consequence, the secondary moment should be included in the design moment. The moment redistribution behavior for symmetrical loading is shown to be quite different from that for unsymmetrical loading. The study also shows that the effect of initial prestress on the moment redistribution is rather important.

Keywords: External tendons; Fiber reinforced polymer; Moment redistribution; Secondary reactions

1. Introduction

External prestressing is a post-tensioning technique in which the prestressing tendons are placed outside a structural element and connected to the structure through anchorages and deviators. Because of its attractive advantages such as fast tendon installation, easy tendon replacement and low friction losses, external prestressing has been broadly used for strengthening and construction of various concrete members.

Fiber reinforced polymer (FRP) composites are being increasingly employed in the field of civil engineering, and many works have been devoted to the study of FRP-reinforced or strengthened structures [1-3]. FRP composites are high-strength and non-corrosive materials with linear elastic property. The elastic modulus of FRP materials covers a wide range, depending on the type of fibers [4]. The FRP modulus of elasticity is usually low, but the elastic modulus for carbon FRP (CFRP) composites can be as high as or even higher than that for the prestressing steel. Among the FRP groups, CFRP composites have been shown to be realistic for substituting the prestressing steel as external tendons, without changing much the overall behavior of the structure [5,6].

In a prestressed continuous member with non-concordant cables [7], it is well known that the prestressing induces secondary reactions and moments. However, there has been a great controversy on the prestress secondary moments (reactions) in the post-elastic range, and no agreement has yet been reached so far. A typical viewpoint is that the secondary moments disappear after the formation of plastic hinges because the continuous beam has become statically determinate. This

viewpoint was included in an early version of the ACI code [8]. On the other hand, in the current version of the ACI code [9], the secondary moments were taken into account in the calculation of the design moments. Some investigators [10] believed that the secondary moments do not change much after the occurrence of cracks. Wyche et al. [11] pointed out that the secondary moments must be considered and that the neglect of secondary moments can be unsafe. In fact, the secondary moments can be beneficial or detrimental, depending on the layout of cables [12]. When a cable is below its linearly transformed concordant line, the secondary moment is beneficial to the support sections but detrimental to the span critical section. The phenomenon is opposite if a cable is above its linearly transformed concordant line.

The redistribution of moments in continuous prestressed concrete members is another topic that has received much interest from researchers [13-15]. The moment redistribution is closely related to the ductility of critical sections. This is reflected by the empirical equations of various codes for calculating the permissible moment redistribution. Most of the codes, including the European and Canadian codes [16,17], adopt the parameter c/d (neutral-axis-to-effective-depth ratio of a section) while the ACI code [9] uses the parameter ε_t (net strain in extreme tension steel). The c/d ratio and the strain ε_t are both ductility-related parameters. Since the common FRP composites are brittle materials with linear elastic behavior up to rupture, the moment redistribution characteristic of external FRP tendon systems may be different from that of conventional concrete members.

This study is conducted to examine the prestress secondary reactions and

redistribution of moment in continuous concrete members prestressed with external CFRP tendons throughout all stages up to the failure load. A numerical test is carried out on two-span continuous beams with test variables including the initial prestress level and the pattern of loading. A previously developed computer model [18] for the nonlinear analysis of externally prestressed beams is used in the study.

2. Numerical test

A numerical test is designed to examine the prestress secondary reactions and the redistribution of moments in continuous concrete beams prestressed with external CFRP tendons. The beams are continuous over two equal spans of 10 m each, and have a rectangular section with 300 mm in width and 600 mm in height, as shown in Fig. 1. Each span is subjected to third-point loads. The loads applied to the right span P_2 are either equal to (symmetrical loading) or 50% of (unsymmetrical loading) the loads applied to the left span $P_1 = P$. The external tendons are draped at deviators that are placed at the center support and third points of each span. The tendon eccentricities at the end supports e_0, outer third point e_1, inner third point e_2 and center support e_3 are 0, 150, 100 and 150 mm, respectively. The external tendons are assumed to be CFRP composites having ultimate strength f_f of 1840 MPa and elastic modulus E_f of 147 GPa. The initial prestress level f_{p0}/f_f varies between 15% and 75%, where f_{p0} is the initial prestress. It should be noted that in practical applications, the initial prestress level in FRP tendons is not possible to go up to 75% because of the stress-rupture phenomenon. Such range of the initial prestress level is just for

comparative purpose of the theoretical study. The tendon area A_p is taken equal to 1000 mm^2. The areas of nonprestressed tensile steel over positive moment region A_{s1} and over negative moment region A_{s2} are 1200 and 800 mm^2, respectively; and the area of nonprestressed compressive steel A_{s3} is taken as 400 mm^2. The yield strength f_y and elastic modulus E_s of nonprestressed steel are 450 MPa and 200 GPa, respectively. The concrete cylinder compressive strength f_{ck} is 60 MPa.

The numerical test is performed using a previously developed finite element model [18]. The model, which was formulated based on the layered Euler-Bernoulli beam theory, is capable of predicting the short-term behavior of externally prestressed concrete beams from prestressing up to failure. The modeling of time-dependent effects was reported elsewhere [19], but the inclusion of these effects will not be covered in this paper. The validity of the model has been verified with the experimental results of a number of specimens available in literature, including both simply-supported beams [20] and continuous beams [12]. In the finite element idealization of the two-span continuous beams shown in Fig. 1, the concrete beam is discretized into 36 beam elements with equal length, and the cross section of the beam element is subdivided into 10 concrete layers and 2 steel layers each of which represents the top or bottom nonprestressed steel. The external tendon is also divided into 36 segments corresponding to the beam elements. The constitutive laws of materials adopted in the present study are as follows:

The stress-strain (σ_c-ε_c) relationship for concrete in compression is simulated using the equation recommended by Eurocode 2 [16], as shown in Fig. 2 (a).

$$\frac{\sigma_c}{f_{cm}} = \frac{k\eta - \eta^2}{1 + (k-2)\eta} \quad (1)$$

where $f_{cm} = f_{ck} + 8$, in MPa; $\eta = \varepsilon_c / \varepsilon_{c0}$; $\varepsilon_{c0}(‰) = 0.7 f_{cm}^{0.31}$; $k = 1.05 E_c \varepsilon_{c0} / f_{cm}$; and $E_c = 22(f_{cm}/10)^{0.3}$, in GPa. The concrete is assumed to be crushed when the concrete strain reaches the ultimate compressive strain, which is equal to 0.003 for f_{ck} = 60 MPa. The stress-strain diagram for concrete in tension is assumed to be composed of a linearly ascending branch before cracking and a linearly descending branch after cracking up to zero stress, as shown in Fig. 2(b). The concrete tensile strength is calculated according to Eurocode 2 [16]. The prestressing FRP tendons are linear elastic up to rupture, as shown in Fig. 2(c). The stress-strain relationship for nonprestressed steel is assumed to be elastic-perfectly plastic in both tension and compression, as shown in Fig. 2(d).

Some typical results (ultimate load P_u, ultimate deflection Δ_u and ultimate stress increase in external tendons Δf_p) for the beams at ultimate are summarized in Table 1. Based on these results, some remarks regarding the general behavior of the beams can be made. (1) unlike the conventional bonded prestressed concrete beams for which the ultimate load-carrying capacity is generally independent of the initial prestress level, the ultimate load-carrying capacity of external CFRP tendon beams increases as the initial prestress increases; (2) a higher initial prestress level leads to a lower ultimate deflection and stress increase in external CFRP tendons; (3) unsymmetrical loading tends to mobilize higher ultimate deflection than symmetrical loading; and (4) due to less development of plastic hinges at the ultimate limit state, unsymmetrical loading produces a significantly smaller stress increase in external tendons and consequently a

lower ultimate load-carrying capacity, compared to symmetrical loading.

3. Secondary reactions

3.1 Proposed method for computing secondary reactions

The response of prestress secondary reactions is identified using a rational method recently developed by the authors [12]. The method is based on the linear transformation concept. Linear transformation is defined as a cable shift over the interior supports of a continuous prestressed concrete member without changing the intrinsic shape of the cable within each individual span [7]. It was stated that the linear transformation of a cable line does not affect the stresses in the concrete and the ultimate load-carrying capacity of a continuous prestressed concrete member [7]. The correctness of this statement has been proved by an experimental work by Aravinthan et al. [10] and more recently by a numerical work by the authors [12]. The general interesting characteristics concerning linear transformation can also be stated as follows [12]: linear transformation causes a change of support reactions and section moments, but it does not change the ultimate load-carrying capacity and the basic flexural behavior (deformations, neutral axis depth and all of the material strains/stresses) over the whole loading process up to the ultimate. In other words, with increasing load up to the ultimate failure, the members with various linearly transformed cables exhibit exactly the same response in all aspects except the support reactions and section moments. The above statement is further confirmed in the current study by performing the analysis of the beams having various linearly

transformed cable lines (the cable profile illustrated in Fig. 1 is linearly transformed into different profiles), but the results are not presented in this paper for limited space.

The method for computing the prestress secondary reactions is illustrated in Fig. 3. Consider a multi-span continuous prestressed concrete member with non-concordant cables. The total reaction at support i, R^i, at any level of loads P consists of two components, namely, the reaction due to external loads R^i_{load} and the secondary reaction due to prestressing R^i_{sec}.

$$R^i = R^i_{load} + R^i_{\text{sec}} \tag{2}$$

The cables can be linearly transformed into a concordant profile, which produces no secondary reactions. Since linear transformation does not influence the flexural characteristics throughout the loading process, the total reaction at support i, $(R^i)_{con}$, for the member with concordant cables, at the load level P, is equal to the load induced reaction R^i_{load} for the member with non-concordant cables.

$$(R^i)_{con} = R^i_{load} \tag{3}$$

Combining Eqs. (2) and (3), the secondary reaction at support i for the member with non-concordant cables can be expressed as follows:

$$R^i_{\text{sec}} = R^i - (R^i)_{con} \tag{4}$$

The support reactions R^i and $(R^i)_{con}$ can be computed by a nonlinear computer analysis, and then the secondary reaction R^i_{sec} is determined according to Eq. (4).

The secondary reactions of a prestressed concrete continuous member should satisfy the following equation:

$$\sum_i R^i_{\text{sec}} = 0 \tag{5}$$

where the summation is made for all the supports. Also, irrespective of the pattern of loading, the secondary reactions at any symmetrical pair of supports i and j, R^i_{sec} and R^j_{sec}, should be equal.

$$R^i_{sec} = R^j_{sec} \tag{6}$$

Eqs. (5) and (6) can be used to check the accuracy and correctness of the proposed method for calculating the secondary reactions.

The proposed method is practically important because it provides a rational approach to compute accurately the secondary reactions and moments in continuous prestressed members over the complete loading range up to failure. The method has been applied only to the external steel tendon beams under symmetrical loading [12]. To better demonstrate the accuracy and applicability of the method and to better understand the behavior of prestress secondary reactions, this newly developed method is applied in the next section to examine the secondary reactions for external CFRP tendon beams, subjected to symmetrical and unsymmetrical loads, having various levels of initial prestress.

3.2 Results

This section presents some details of the computation and the results of secondary reactions and support reactions for two-span continuous external CFRP tendon beams shown in Fig. 1. To compute the secondary reactions using the aforementioned method, the linearly transformed concordant profile of external tendons should be determined first. This concordant cable line is obtained using a trial-and-error method by performing a series of analyses of linearly transformed tendon beams subjected to

the prestressing force (neglecting the weight of the beams and external loads). The cable line is constantly adjusted until the support reactions disappear. The original non-concordant cables and linearly transformed concordant cables are shown in Fig. 4. Linear transformation is made by shifting the original cable line over the center support by Δ, and correspondingly by (2Δ)/3 over the inner third point and Δ/3 over the outer third point, as illustrated in the figure. It is demonstrated that the linearly transformed concordant cable line for the initial prestress level of 75% is slightly different from that for lower initial prestress levels. For the former the cable shift at the center support Δ = 45.26 mm, while for the latter Δ = 45.39 mm. This can be explained that the 75% initial prestress level mobilizes an obviously larger axial shortening of the beam, thereby causing a slight difference of the cable line, when compared to lower initial prestress levels.

The development of support reactions and the evolution of secondary reactions at end and center supports for symmetrical loading are shown in Fig. 5, while the results for unsymmetrical loading are shown in Fig. 6. In the figures, R^1, R^2, an R^3 represent respectively the reactions at left, intermediate and right supports for the beams analyzed; $(R^1)_{con}$, $(R^2)_{con}$, and $(R^3)_{con}$ are those for the beams with linearly transformed concordant cables; and R^1_{sec} $(= R^1 - (R^1)_{con})$, R^2_{sec} $(= R^2 - (R^2)_{con})$ and R^3_{sec} $(= R^3 - (R^3)_{con})$ are secondary reactions at left, intermediate and right supports, respectively. It is seen that the support reactions develop linearly with the applied load up to the appearance of flexural cracks. Beyond that, the reaction development exhibits nonlinear behavior due to redistribution of moments. In addition, this

nonlinear behavior is more obvious for a lower prestress level compared to a higher prestress level, and for symmetrical loading compared to unsymmetrical loading, attributed to more significant redistribution of moments (to be discussed later). The response of prestress secondary reactions with the applied load is characterized by three stages with two turning points corresponding to concrete cracking and steel yielding, respectively. This observation is different from some points of view which deemed that the secondary reactions (moments) would remain unchanged, decrease or disappear after the appearance of cracks or after the formation of plastic hinges (yielding of steel). In contrast, the present study indicates that the secondary reactions increase quicker after cracking or yielding, attributed to quicker increase in the prestressing force.

From Figs. 5 and 6, it can be observed that the secondary reactions at any stage of loading, obtained from the proposed method, satisfy the calibration equations indicated by Eqs. (5) and (6). For symmetrical loading, the secondary reaction at the center support is twice in magnitude and opposite in direction compared to the secondary reaction at the end support. For unsymmetrical loading, the secondary reaction at the left support is the same as that at the right support, and the summation of the secondary reactions at all three supports is zero. A very slight error at high levels of loading can be attributed to a slight change of the linearly transformed concordant cable line, caused by additional shortening of the beams as a result of external loads.

Figs. 7 and 8 illustrate the variation of the secondary reaction with the tendon

stress for symmetrical loading and unsymmetrical loading, respectively. It is seen that there is a linear relationship between the secondary reaction at a support and the tendon stress. The diagrams for various initial prestress levels are in a same straight line which crosses the zero point. Irrespective of the pattern of loading, the line slopes for the center and end supports are -9.08 and 4.54 N/MPa, respectively. It should be noted that the slope depends on the cable deviation from the linearly transformed concordant line. The larger the deviation, the steeper the slope.

At the ultimate limit state, the secondary moments in the beams under symmetrical and unsymmetrical loading are shown in Figs. 9 and 10, respectively, where X/L is the ratio of the distance from the end support to the span. Because the reaction at the end support is positive, the secondary moments produced by the support reaction are also positive over the beam. As a consequence, they counteract the negative moment at the center support while accentuate the positive moment at the span critical section. Because the cable line is rather close to the linearly transformed concordant line as illustrated in Fig. 4, the prestress secondary moments are not so important. If the cable deviation from the linearly transformed concordant line is larger, the secondary moments would be more important.

4. Moment redistribution

4.1 Development of moments and moment ratio

For continuous prestressed concrete members subjected to dead and live loads, the total moment M of a section is composed of the following contributions:

$$M = M_L + M_D + M_{\text{sec}} \tag{7}$$

in which M_L is the moment caused by live loads (live moment); M_D is the moment caused by dead loads (dead moment) and M_{sec} is the moment caused by prestressing (secondary moment).

Denote by M_{L1} and M_{L2} the live moments at the span critical section and at the center support, respectively. Based on the elastic theory, the value of the moment ratio $(M_{L2}/M_{L1})_{ela}$ remains constant with varying load. However, the actual value of the moment ratio M_{L2}/M_{L1} is subject to changes when the redistribution of moments takes place. Therefore, it would be interesting to observe the moment redistribution behavior in terms of the evolution of this moment ratio. According to Eq. (7), the live moment can be obtained from: $M_L = M - M_D - M_{\text{sec}}$, where the secondary moment M_{sec} is calculated according to the secondary reaction obtained by the method mentioned in the previous section.

Figs. 11 and 12 show the variation of the moment ratio as well as the live moments for symmetrical loading and unsymmetrical loading, respectively. The values of $(M_{L2}/M_{L1})_{ela}$ for symmetrical loading and unsymmetrical loading are 1.48 and 0.99, respectively. Prior to cracking, there is no redistribution of moments and, therefore, the moments develop linearly with the applied load and the value of M_{L2}/M_{L1} is also equal to 1.48 (for symmetrical loading) or 0.99 (for unsymmetrical loading), as expected. After cracking, the moment redistribution takes place. As a consequence, the load-moment relationship displays nonlinear behavior and the value of M_{L2}/M_{L1} deviates from the constant value. The evolution of the ratio M_{L2}/M_{L1}

is intimately related to the progress of moment redistribution, and is influenced by several phases, typically the yielding of bonded steel (also termed as the formation of plastic hinges) as marked in the graph. Detailed discussions on the moment redistribution will be presented in the next section.

4.2 Degree of moment redistribution

The amount of moment redistribution can be measured in terms of the degree of redistribution β:

$$\beta = 1 - (M_e / M) \tag{8}$$

where M_e is the elastic moments calculated from an elastic analysis by assuming that the constituent materials are linear elastic; and M is the actual moments obtained from the nonlinear finite element analysis.

Figs. 13 and 14 illustrate the evolution of the degree of moment redistribution at center support and span critical section for symmetrical loading and for unsymmetrical loading, respectively. It is seen that at initial loading up to the cracking load, the degree of moment redistribution is equal to zero. In this stage, the actual moments are equal to the elastic values and the moment redistribution does not yet take place. In addition, the higher the initial prestress, the higher the cracking load corresponding to the commencing of moment redistribution. After cracking the evolution of moment redistribution is affected by some phases, and the evolution for symmetrical loading is different from that for unsymmetrical loading, as can be seen in the figures.

For the beams under symmetrical loading, the redistribution of moments is

positive at the center support and, correspondingly, negative at the span critical section. The degree of redistribution increases quickly with the development of cracks and the rate of increase for a lower initial prestress level is greater than that for a higher one. When the crack development stabilizes, the evolution of redistribution reaches a plateau, which however is not so stable for the 15% initial prestress level. After the steel at the center support begins to yield, the degree of moment redistribution resumes a quick increase until the steel at the span critical section yields. Beyond that, the degree of moment redistribution tends to decreases slightly for low prestress levels (15% and 35%) or increases gradually for normal (55%) and high (75%) prestress levels.

For the beams under unsymmetrical loading, the redistribution of moments at the center support during loading may be positive, negative, or changeable from a negative value to a positive value, depending on the prestress level. In these beams, the first crack appears at the span critical section except for the beam with a 15% initial prestress level, in which the first crack appears at the center support as in the case of symmetrical loading. As a consequence, upon cracking the moments are redistributed from the span critical section towards the center support, leading to negative redistribution over the center support (correspondingly positive redistribution over the span critical section), except for the beam with a 15% initial prestress level, in which the phenomenon is opposite. Once the crack development stabilizes, the moments turn to redistributed from the lower reinforced center support section to the heavier reinforced span critical section, leading to a gradual growth in the degree of

redistribution at the center support section. For the 15% initial prestress level, a plateau occurs subsequently, whereas for higher initial prestress levels there is no such plateau. When the first plastic hinge forms, a quicker increase in the degree of moment redistribution at the center support section is observed for low prestress levels (15% and 35%), while the change in the redistribution for normal (55%) and high (75%) prestress levels is not obvious. This is attributed to that, for the low prestress levels, the first plastic hinge appearing at the center support is obviously earlier than the second plastic hinge forming at the span critical section, while for the normal or high prestress level, the formations of the first and second plastic hinges are very close, as can be seen in Fig. 12.

Fig. 15 shows the variation of the degree of moment redistribution with the neutral axis dept for the center support section of the beams under symmetrical loading. The higher the initial prestress, the higher the neutral axis depth at first cracking which is corresponding to the beginning of the moment redistribution. It is generally observed that at a given prestress level, the degree of moment redistribution increases quickly with the decrease of the neutral axis depth. However, the increasing moment redistribution with decreasing neutral axis depth is not consistent. On stabilization of crack development and on second yielding, as marked in the graph, the degree of the moment redistribution decreases for the 15% initial prestress level or remains almost unchanged for higher initial prestress levels as the neutral axis depth decreases.

Fig. 16 demonstrates the variation of the degree of moment redistribution for the center support section with the initial prestress level. For symmetrical loading, the

data at first yielding, second yielding and ultimate are presented. The redistribution at first yielding can be considered as the redistribution at service conditions, because there is a fairly long plateau prior to first yielding, as illustrated in Fig. 13. It is seen that the redistribution decreases as the initial prestress increases. The degrees of redistribution at first yielding are about 50% of the corresponding values at ultimate. The degrees of redistribution at second yielding are a little higher at a low prestress level whereas a little lower at a normal or high prestress level than the redistribution at ultimate. It is also observed that the redistribution for unsymmetrical loading is substantially lower than that for symmetrical loading. This can be attributed to the combined effects of the load pattern and the stiffness difference between negative and positive moment regions. For unsymmetrical loading, the moments are prone to redistributed from the span critical section to the center support which is usually non-critical. Meanwhile, the moments are also prone to redistributed from the lower reinforced center support section to the higher reinforced midspan section. Therefore, the effects of the pattern of loading counteract the effects of the steel arrangement, leading to low redistribution of moments for unsymmetrical loading. Based on the above discussions, it can be deduced that, if the center support section is stiffer than the span critical section, the beams under unsymmetrical loading would exhibit high redistribution of moments (negative redistribution at the center support) because in this case this pattern of loading accentuates the effects of the stiffness difference.

5. Conclusions

A numerical investigation has been carried out on two-span continuous concrete beams prestressed with external CFRP tendons to identify the prestress secondary reactions and redistribution of moments in such type of members. The following conclusions can be drawn:

- The proposed method, which is based on the linear transformation concept combined with a powerful nonlinear computer analysis program, can predict accurately the secondary reactions (moments) of continuous external tendon beams at all stages of loading.
- The secondary reactions for a beam with non-concordant cables are present throughout the loading process. Since the complete development of plastic hinges is not likely to happen for external FRP tendon systems in engineering practices, the inclusion of the secondary moment is necessary when calculating the design moment of this structural typology.
- After cracking, the moment development displays nonlinear behavior and the value of M_{L2} / M_{L1} deviates from the elastic constant value due to redistribution of moments. The results show that there is a very close relationship between the evolution of M_{L2} / M_{L1} and the progress of moment redistribution.
- The development of moment redistribution for symmetrical loading is shown to be quite different from that for unsymmetrical loading. The level of initial prestress is found to have important influence on the moment redistribution in continuous concrete beams prestressed with external CFRP tendons.

Acknowledgments

This research is sponsored by FEDER funds through the program COMPETE – Programa Operacional Factores de Competitividade – and by national funds through FCT – Fundação para a Ciência e a Tecnologia –, under the project PEst-C/EME/UI0285/2013. The work presented in this paper has also been supported by FCT under Grant No. SFRH/BPD/66453/2009.

References

[1] Al-Sunna R, Pilakoutas K, Hajirasouliha I, Guadagnini M. Deflection behaviour of FRP reinforced concrete beams and slabs: An experimental investigation. Composites Part B 2012; 43: 2125-2134.

[2] Caporale A, Feo L, Luciano R. Limit analysis of FRP strengthened masonry arches via nonlinear and linear programming. Composites Part B 2012; 43: 439-446.

[3] Seo SY, Feo L, Hui D. Bond strength of near surface-mounted FRP plate for retrofit of concrete structures. Composite Structures 2013; 95: 719-727.

[4] Fib. Model Code 2010. Bulletins 55 and 56, International Federation for Structural Concrete (fib), Lausanne, Switzerland; 2012.

[5] Lou TJ, Lopes SMR, Lopes AV. Numerical analysis of behaviour of concrete beams with external FRP tendons. Construction and Building Materials 2012; 35: 970-978.

[6] Bennitz A, Schmidt JW, Nilimaa J, Taljsten B, Goltermann P, Ravn DL. Reinforced concrete T-beams externally prestressed with unbonded carbon fiber-reinforced polymer tendons. ACI Structural Journal 2012; 109(4): 521-530.

[7] Lin TY, Burns NH. Design of prestressed concrete structures. John Wiley & Sons, New York; 3rd Edition, 1981.

[8] ACI Committee 318. Building code requirements for reinforced concrete (ACI 318-71). American Concrete Institute, Farmington Hills, MI; 1971.

[9] ACI Committee 318. Building code requirements for structural concrete (ACI 318-11) and commentary. American Concrete Institute, Farmington Hills, MI; 2011.

[10] Aravinthan T, Witchukreangkrai E, Mutsuyoshi H. Flexural behavior of two-span continuous prestressed concrete girders with highly eccentric external tendons. ACI Structural Journal 2005; 102(3): 402-411.

[11] Wyche PJ, Uren JG, Reynolds GC. Interaction between prestress secondary moments, moment redistribution, and ductility – A treatise on the Australian concrete codes. ACI Structural Journal 1992; 89(1): 57-70.

[12] Lou TJ, Lopes SMR, Lopes AV. Flexural response of continuous concrete beams prestressed with external tendons. ASCE Journal of Bridge Engineering 2013; 18(6): 525-537.

[13] Lopes SMR, Harrop J, Gamble AE. Study of moment redistribution in prestressed concrete beams. ASCE Journal of Structural Engineering 1997; 123(5): 561-566.

[14] Kodur VKR, Campbell TI. Factors governing redistribution of moment in

continuous prestressed concrete beams. Structural Engineering and Mechanics 1999; 8(2): 119-136.

[15] Zhou W, Zheng WZ. Experimental research on plastic design method and moment redistribution in continuous concrete beams prestressed with unbonded tendons. Magazine of Concrete Research 2010; 62(1): 51-64.

[16] CEN. EN 1992-1-1. Eurocode 2: Design of concrete structures – Part 1-1: General rules and rules for buildings. European Committee for Standardization, Brussels, Belgium; 2004.

[17] Canadian Standards Association. Design of concrete structures (A23.3-04). Mississauga, Ontario, Canada; 2004.

[18] Lou TJ, Xiang YQ. Finite element modeling of concrete beams prestressed with external tendons. Engineering Structures 2006; 28(14): 1919-1926.

[19] Lou TJ, Lopes SMR, Lopes AV. Nonlinear and time-dependent analysis of continuous unbonded prestressed concrete beams. Computers & Structures 2013; 119: 166-176.

[20] Lou TJ, Lopes AV, Lopes SMR. Influence of span-depth ratio on behavior of externally prestressed concrete beams. ACI Structural Journal 2012; 109(5): 687-695.

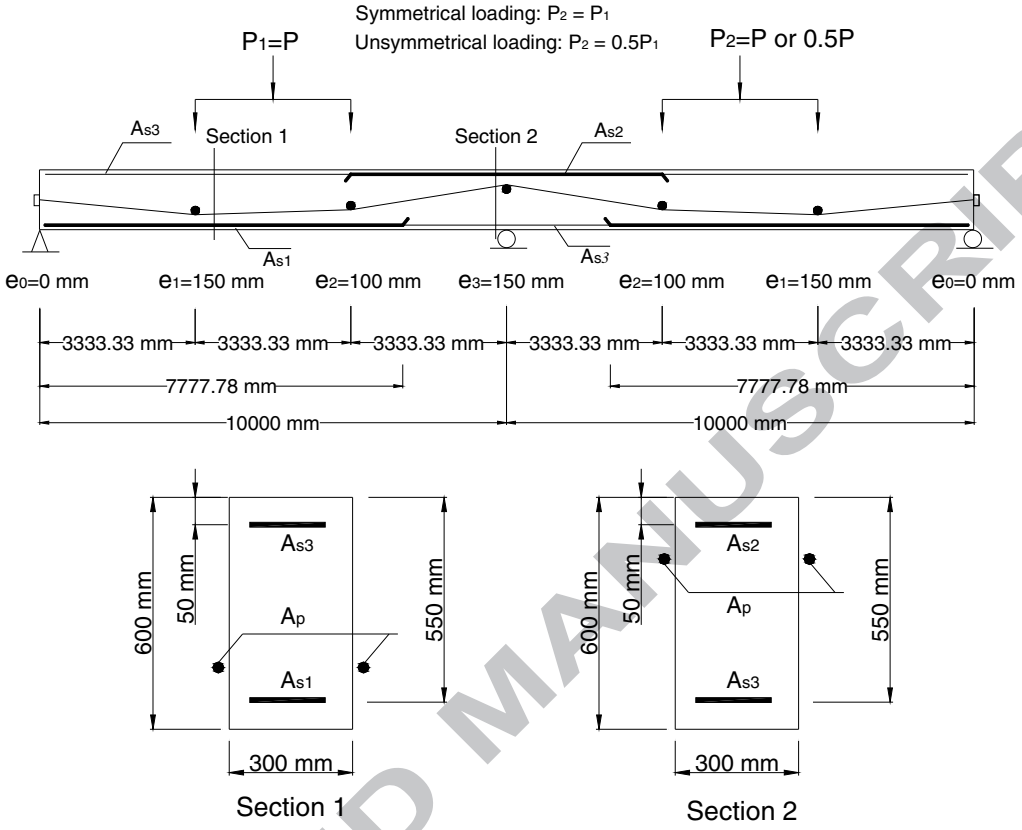

Fig. 1 Details of the beams used for the analysis

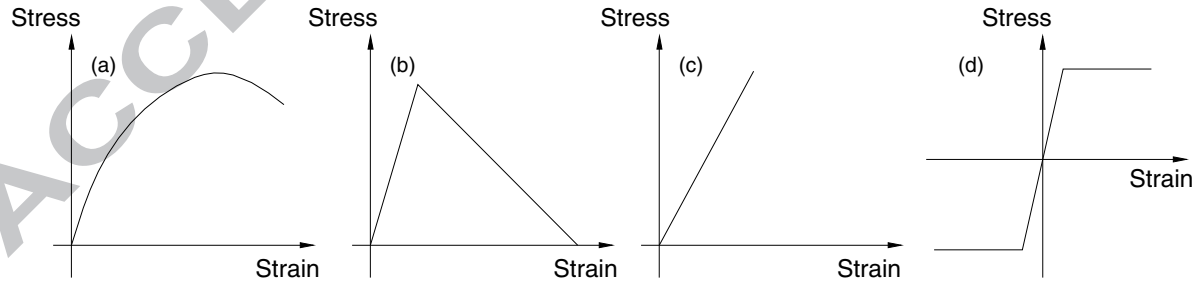

Fig. 2 Schematic diagrams of material stress-strain laws. (a) concrete in compression; (b) concrete in tension; (c) CFRP tendons; (d) nonprestressed steel

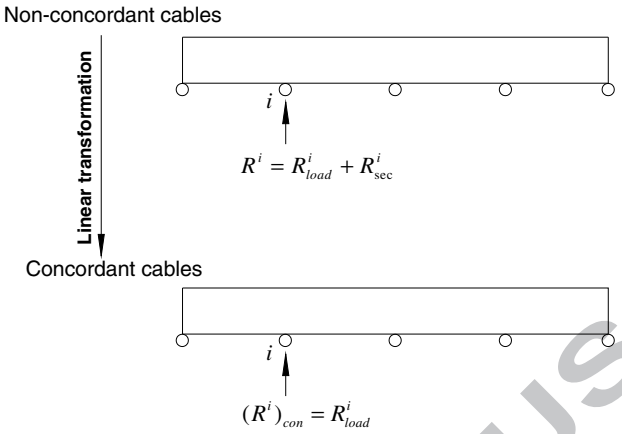

Fig. 3 Support reactions for beams with non-concordant and linearly transformed concordant cables

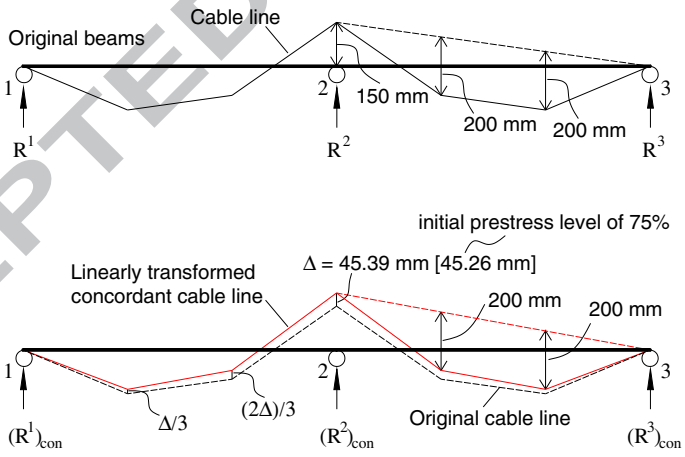

Fig. 4 Original beams with non-concordant cables and linearly transformed beams with concordant cables

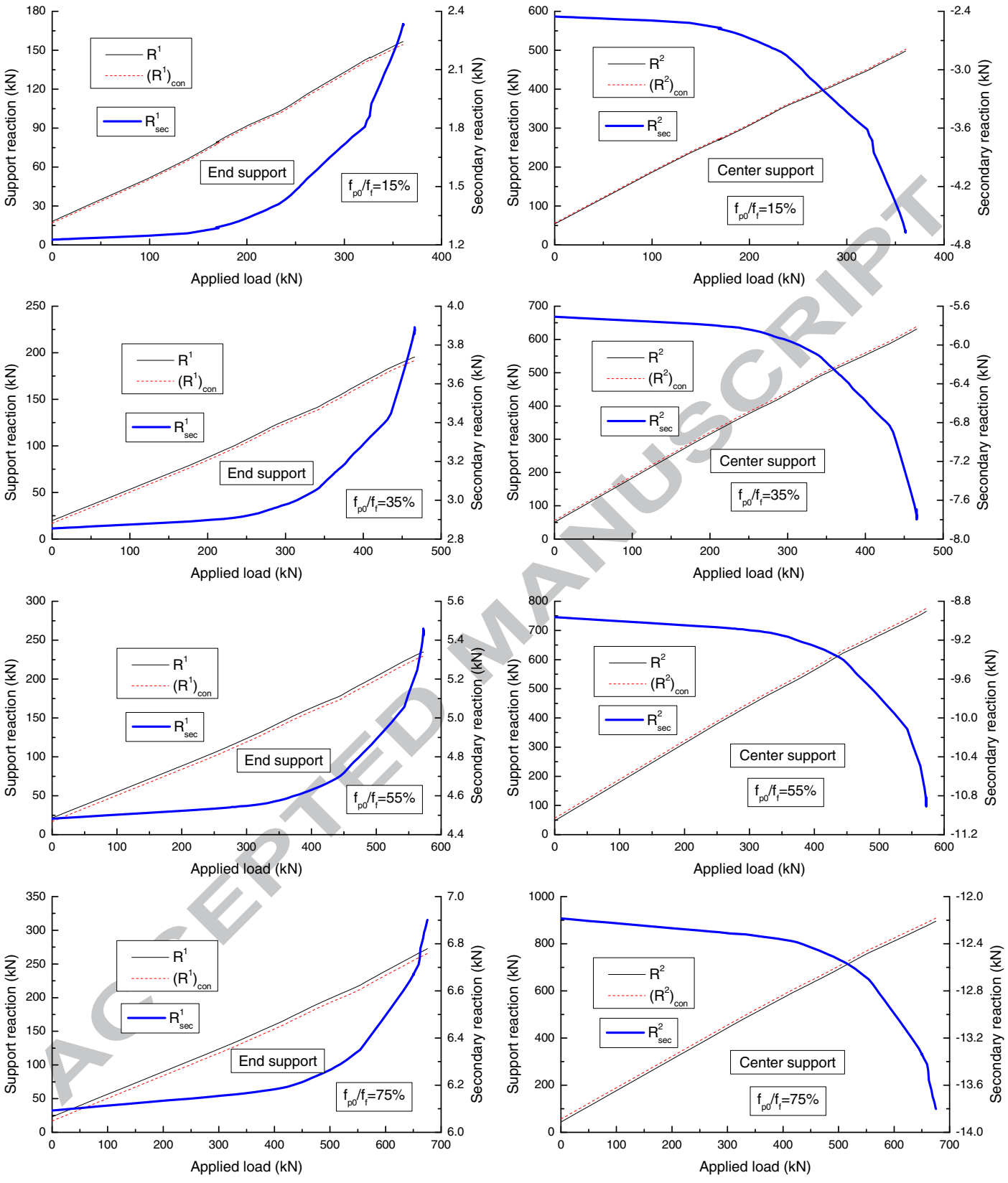

Fig. 5 Development of support reactions and secondary reactions for the beams under symmetrical loading

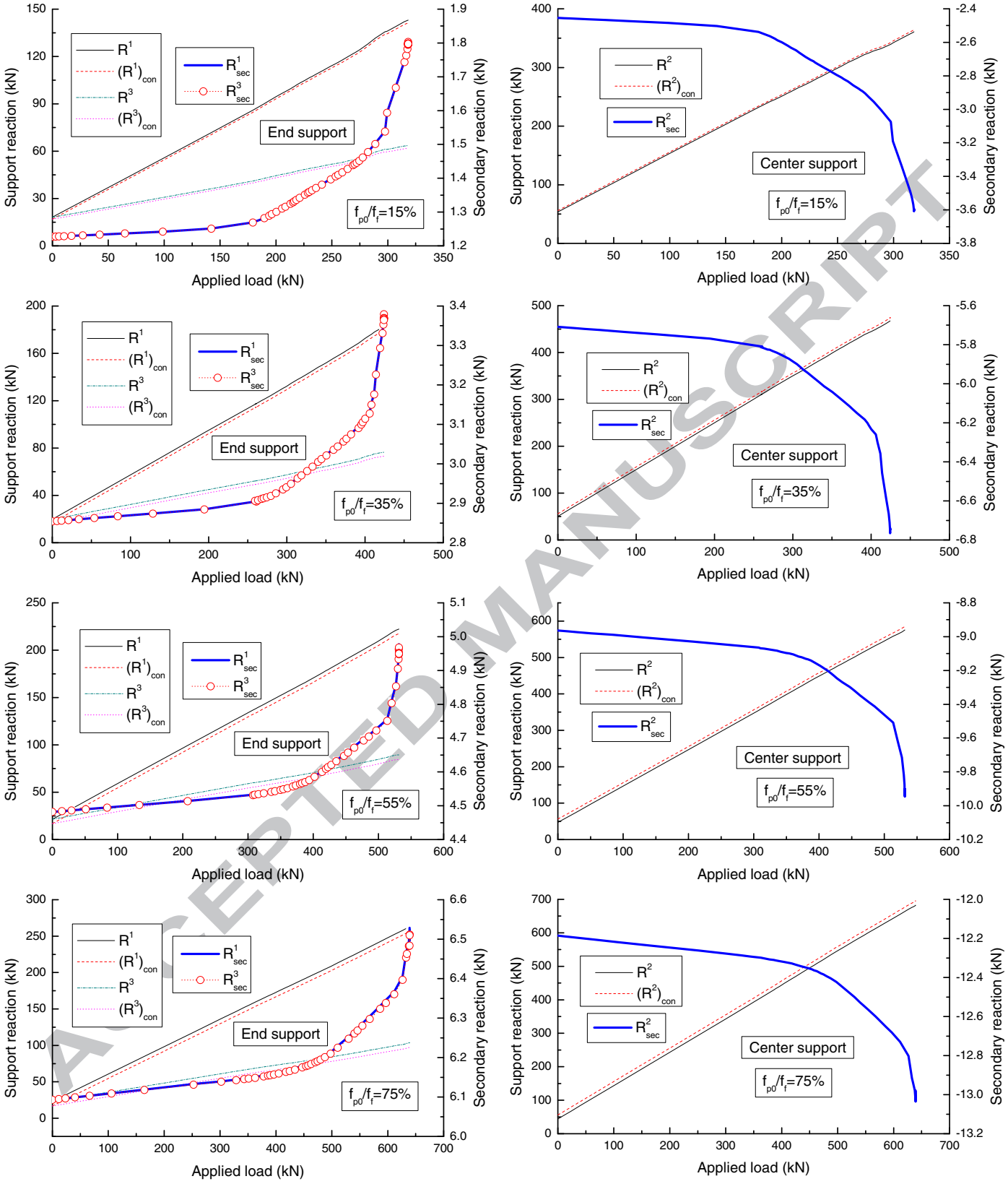

Fig. 6 Development of support reactions and secondary reactions for the beams under unsymmetrical loading

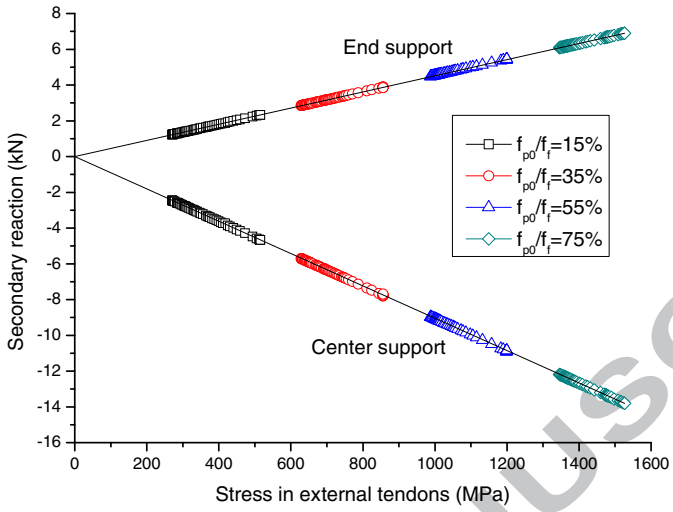

Fig. 7 Variation of secondary reactions with the stress in external tendons for the beams under symmetrical loading

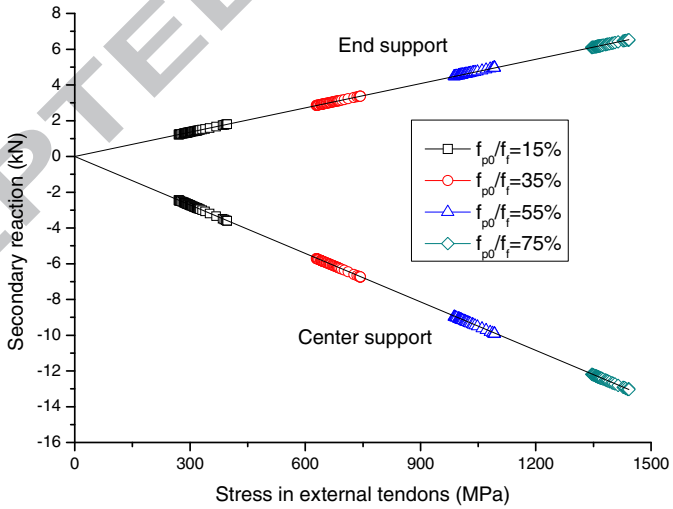

Fig. 8 Variation of secondary reactions with the stress in external tendons for the beams under unsymmetrical loading

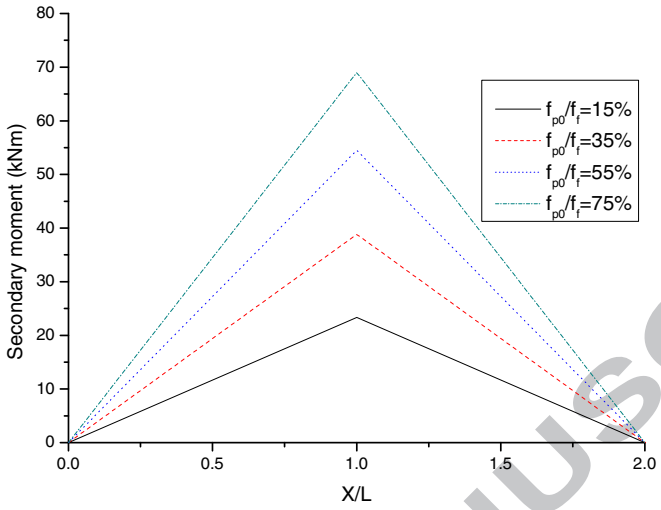

Fig. 9 Secondary moments in the beams under symmetrical loading at ultimate

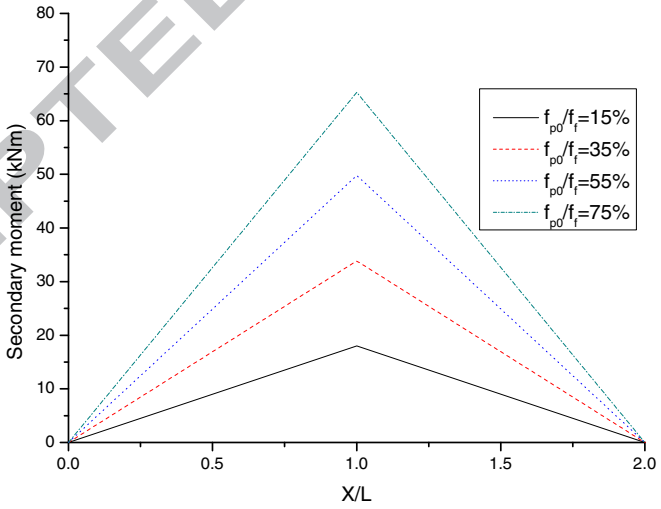

Fig. 10 Secondary moments in the beams under unsymmetrical loading at ultimate

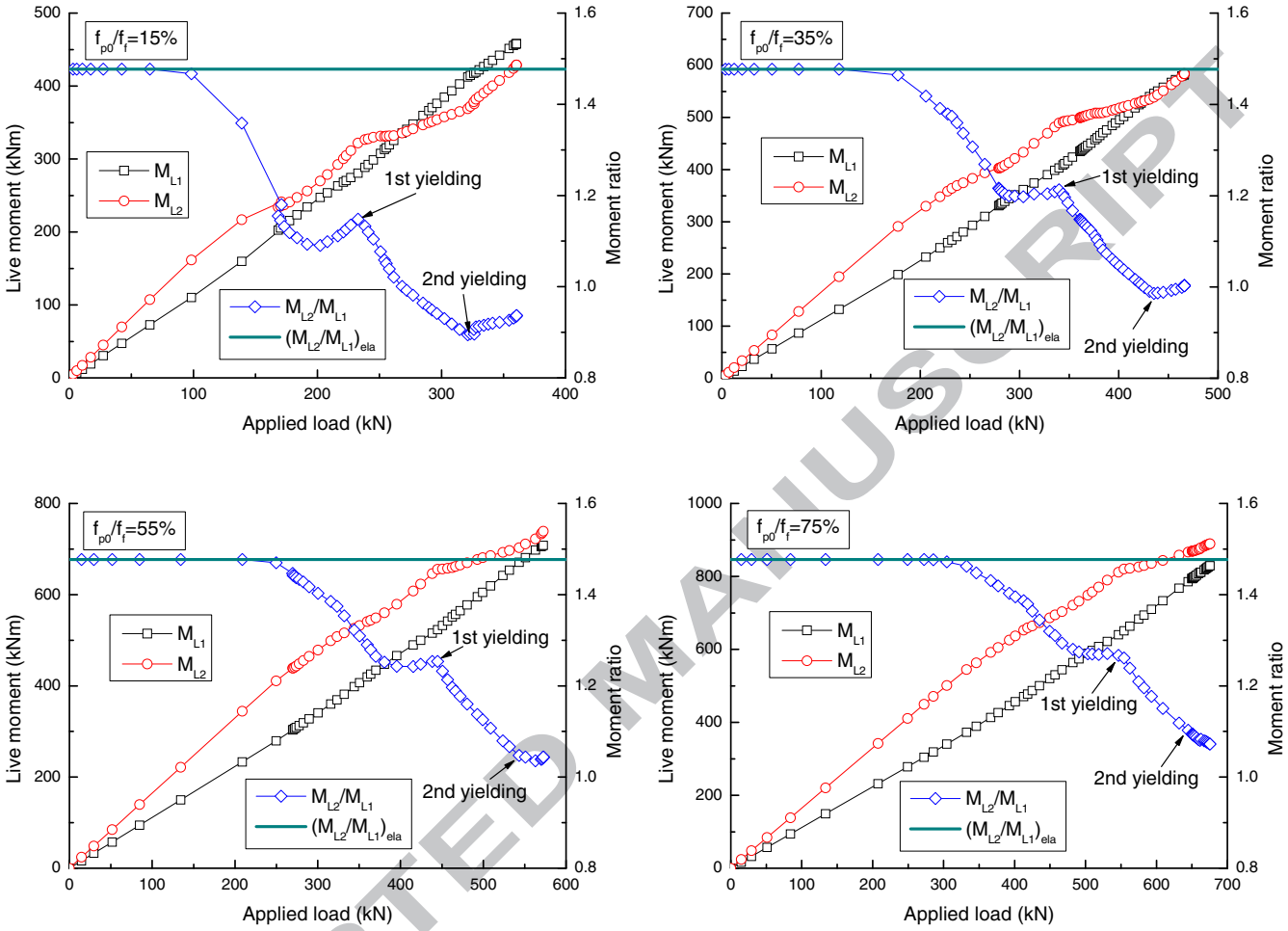

Fig. 11 Development of live moments and moment ratios for the beams under symmetrical loading

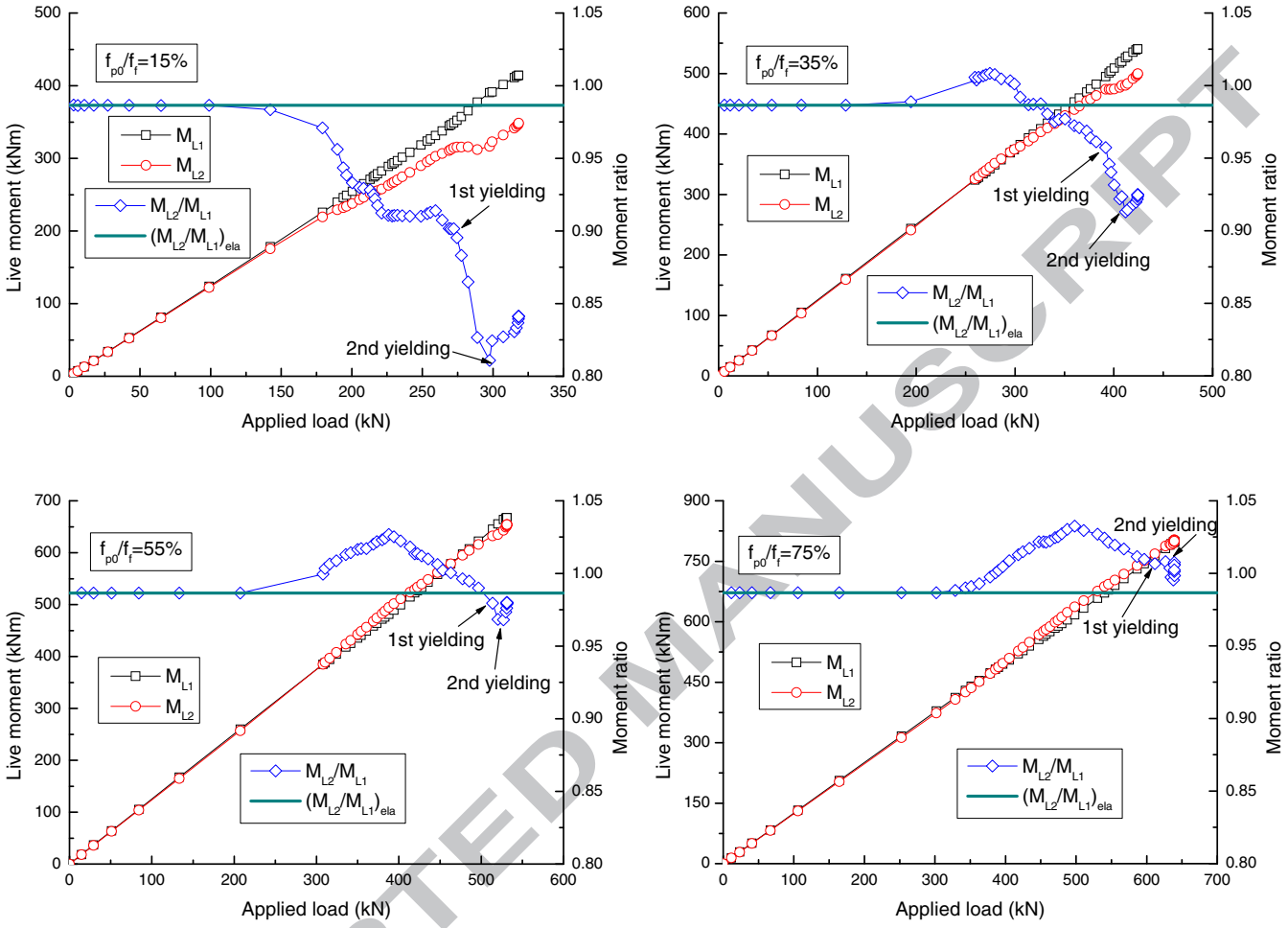

Fig. 12 Development of live moments and moment ratios for the beams under unsymmetrical loading

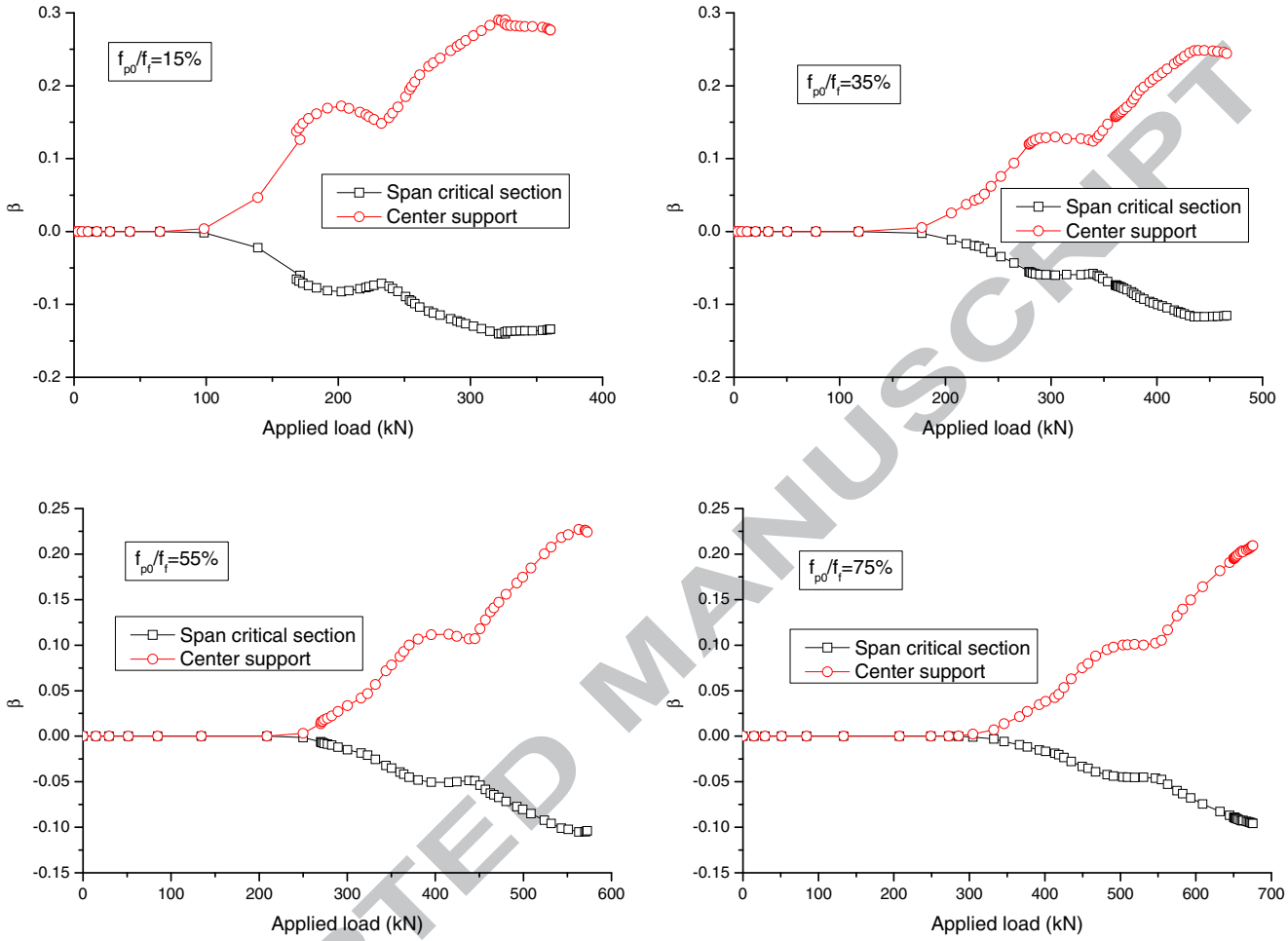

Fig. 13 Variation of the degree of moment redistribution with applied load for the beams under symmetrical loading

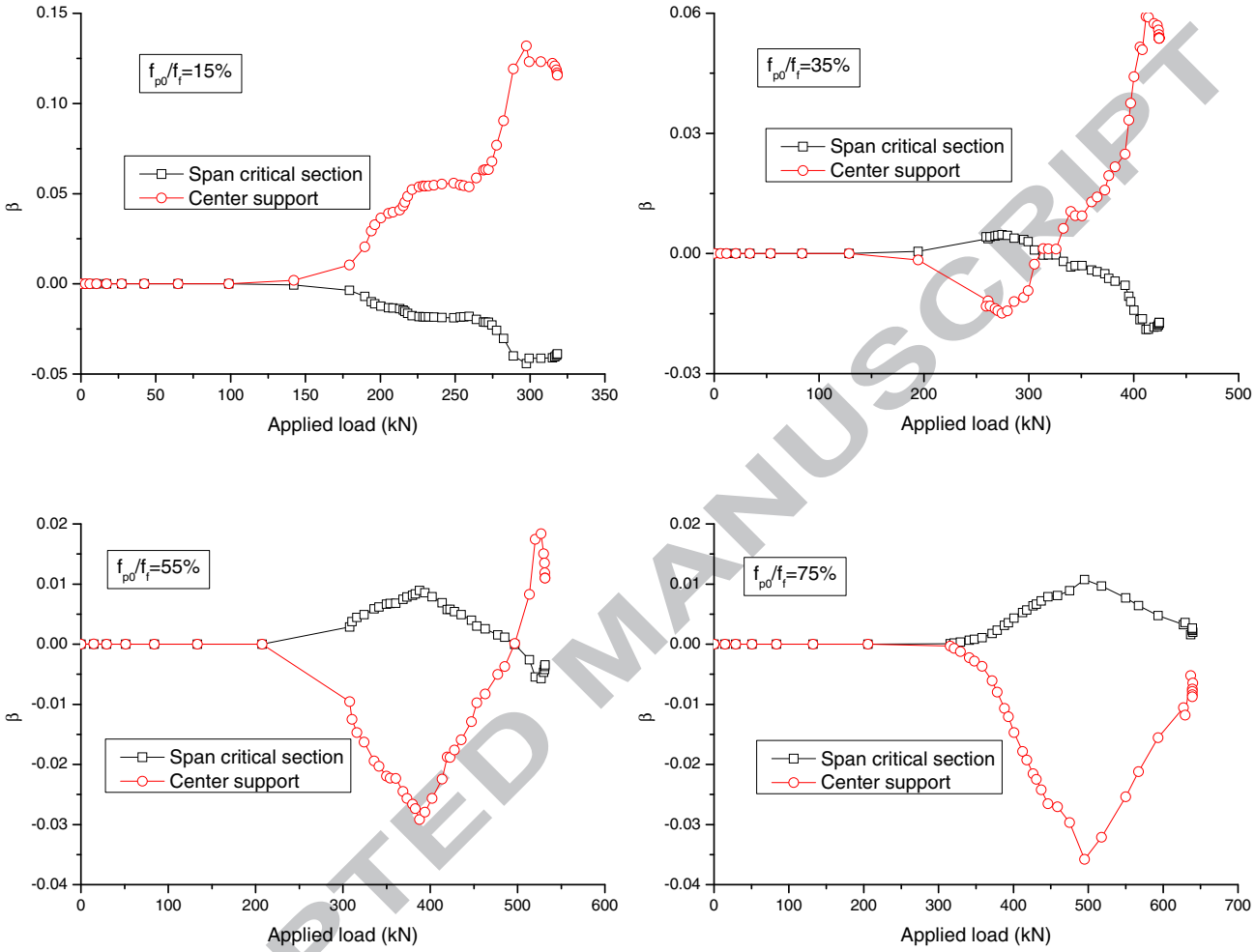

Fig. 14 Variation of the degree of moment redistribution with applied load for the beams under unsymmetrical loading

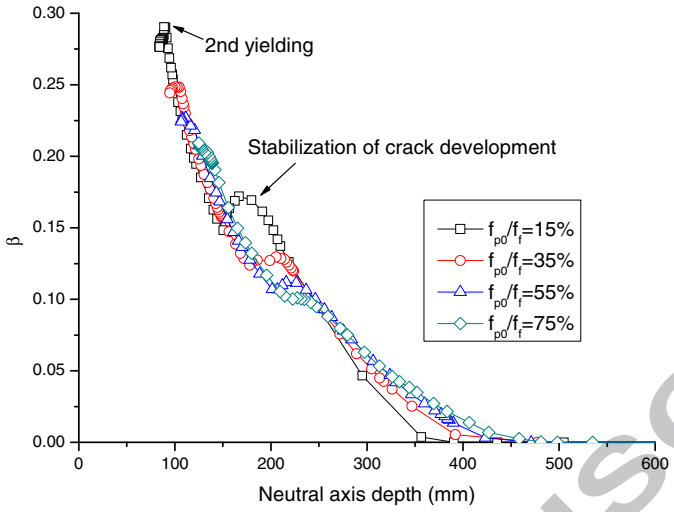

Fig. 15 Variation of the degree of moment redistribution with neutral axis depth for center support section of the beams under symmetrical loading

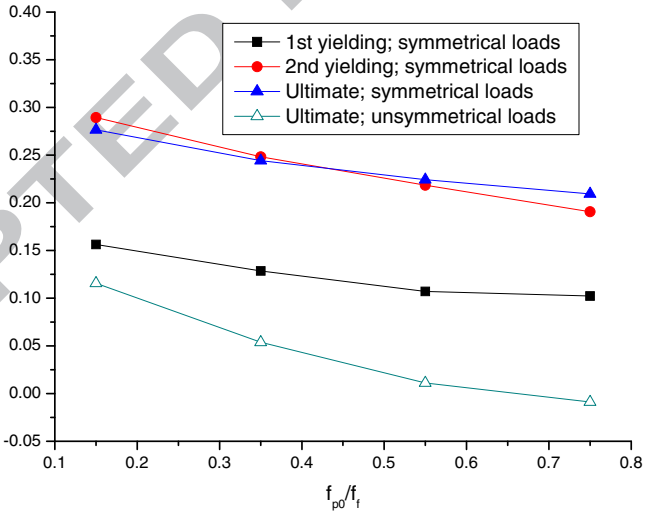

Fig. 16 Variation of the degree of moment redistribution at center support with initial prestress level

Table 1 Typical results for the beams at ultimate

P_2/P_1	f_{p0}/f_f	P_u (kN)	Δ_u (mm)	Δf_p (MPa)
1.0	15%	360.53	77.08	244.90
	35%	465.99	74.14	227.11
	55%	572.61	71.78	212.06
	75%	675.43	64.63	180.79
0.5	15%	318.29	80.54	126.59
	35%	424.24	77.18	115.00
	55%	531.37	74.74	105.49
	75%	639.08	72.63	96.77